NEXAFS Studies on the Surface Orientation of Buffed Polyimides

M. G. Samant, J. Stöhr, H. R. Brown,‡ and T. P. Russell*,†

IBM Research Division, Almaden Research Center, 650 Harry Road, San Jose, California 95120

J. M. Sands and S. K. Kumar

Department of Materials Science and Engineering, The Pennsylvania State University, University Park, Pennsylvania 16802

Received December 11, 1995; Revised Manuscript Received March 11, 1996[⊗]

ABSTRACT: Near-edge X-ray absorption fine structure (NEXAFS) spectroscopy has been used to determine the average near-surface orientation of chains in a buffed polyimide film. Auger and total electron yield measurements provide powerful and direct means of determining the orientation of chains as a function of depth. In the case of a strongly buffed sample, the polyimide chains at the film surface are found to be highly aligned along the buffing direction. We also find significant alignment of the phenyl ring planes parallel to the surface. The alignment is discussed in terms of simple models that are useful in visualizing the alignment in partially disordered systems. The chain orientation decays as a function of distance from the surface, becoming random in the bulk. The 1/e alignment depth is ≃100 Å. Studies as a function of load applied during buffing and distance of buffing show that the near-surface orientation saturates at relatively small loads and short distances. The 1/e buffing load and buffing distance for the near-surface alignment are 1.2 g/cm^2 and 67 cm, respectively.

Introduction

An essential component in flat panel displays is a thin (≃0.2 μm) film of an aromatic polyimide, coated onto an electrode surface, that is uniaxially rubbed with a velour cloth.[1] Placing a liquid crystal in contact with the rubbed surface results in a monodomain alignment of the liquid crystal in the direction of rubbing.[2−6] The tilt angle of the liquid crystal with respect to the substrate and the strength of anchoring the liquid crystal to the substrate depend strongly on the chemical nature of the polymer and the buffing conditions. Until recently, the action of buffing on the polymer film and the origin of the liquid crystal alignment were poorly understood. Grazing incidence X-ray scattering studies clearly demonstrated that the polyimide chains near the surface were markedly aligned during the buffing.[7] If one considers that the glass transition temperature, T_g, of the polyimide is in excess of 350 °C,[8] that the buffing is done at room temperature, and that the load applied for buffing is rather small (≃2 g/cm^2), it is remarkable that any orientation occurs. The fact that orientation of the near-surface chains is found and that this orientation propagates at most 100 Å into the film suggests that the mechanical properties of the chains at the surface are much different from those in the bulk. This difference may in fact be associated with a marked reduction in the entanglement density of chains in the vicinity of the surface,[9] a near-surface glass transition temperature that is different from that of the bulk,[10−12] or very high local strains during the buffing. However, a better definition of the buffing conditions and the depth dependence of the orientation are necessary to gain a more quantitative understanding of this process.

Near-edge X-ray absorption fine structure (NEXAFS) spectroscopy offers a unique means of probing the near-surface structure and orientation of polymers. Near the K-shell absorption threshold, NEXAFS spectra are dominated by resonances arising from transitions from the 1s core level to unfilled molecular orbitals of π^* and σ^* symmetry.[13] Since such states are specific to the bonding within different functional groups, NEXAFS can be used to probe the chemical composition of materials. This fact has been used, for example, to probe lateral compositional inhomogeneities in thin polymer films with high spatial resolution.[14] In electron yield detection, the NEXAFS signal originates from the near-surface region of the sample. Two commonly used methods are Auger electron yield (AEY) or total electron yield (TEY) detection,[13] which at the carbon K-edge give sampling depths of about 10 and 100 Å, respectively.[15] Thus, the various electron yield detection methods provide a unique tool for probing compositional variations near a surface with exceptional depth resolution. The intensity of the NEXAFS resonances depends on the nature and filling of the molecular orbitals and on the included angle between the electric field vector of the X-rays, $\vec{E}$, and the direction of the valence orbitals.[13] Since synchrotron radiation is nearly linearly polarized, NEXAFS offers a powerful means of examining the orientation of bonds within polymer chains. In the case of buffed polymer films, the orientation of polymer chain segments at the surface will, of course, result in an anisotropy in the orientation of bonds within the chains. This anisotropy will be quantitatively reflected in the variation of resonance intensities as the sample orientation is changed relative to the fixed direction of $\vec{E}$.[16] The orientation of the polymer chain, defined as the average orientation of the chain segments, is then determined from that of the bonds in the various functional groups. Similar to other spectroscopies, such as infrared or Raman, a dichroic ratio which is related to the orientation of the polymer can be defined. By using either the Auger or total electron yield, the depth dependence of the chain orientation can be directly measured.

Herein, NEXAFS is used to investigate the orientation of an aromatic polyimide as a function of distance from the surface. Measurements of NEXAFS as a function of X-ray incidence angle provide insight into the conformation of the polyimide chain relative to the

† Current address: Polymer Science and Engineering, University of Massachusetts, Amherst, MA 01003.
‡ Current address: BHP Institute for Steel Processing, University of Wollongong, Australia.
⊗ Abstract published in *Advance ACS Abstracts,* November 1, 1996.

S0024-9297(95)01820-1 CCC: $12.00

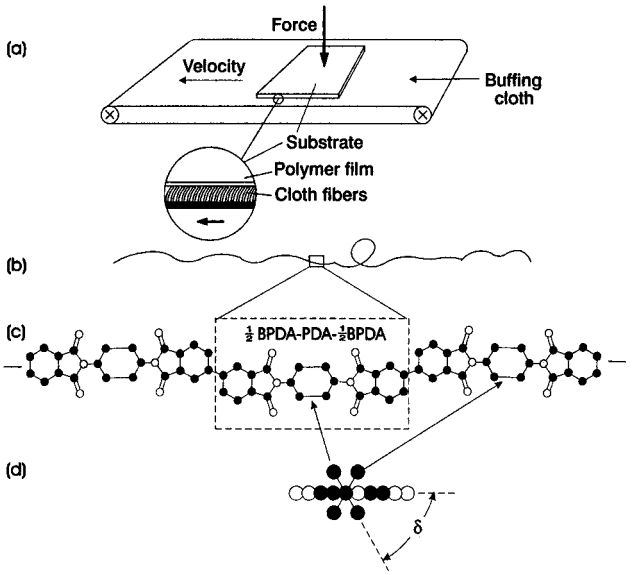

Figure 1. (a) Schematic of the buffing process. The shaded rectangle represents the sample pressed by a force against the velour cloth, which is represented by the bristled surface. The velour cloth is moved at a constant velocity for the desired buffing distance. (b) Picture of a polyimide chain, consisting of rigid monomer units shown in the dashed box with a flexible linkage between them, as illustrated in (c). Here we show the structure of BPDA−PDA polyimide in the fully stretched configuration. In this case the chain axis is parallel to the monomer axis and the π orbitals of all phenyl rings and the C═O unit are perpendicular to the chain axis. (d) View of the fully stretched polyimide chain along the chain axis, showing that the plane of the PDA groups is rotated about the chain axis by $\delta = 60°$ relative to the plane of the BPDA groups.

surface plane and the buffing direction. It is shown that the orientation near the surface is much greater than the average orientation of chains within the first 100 Å. This result is in agreement with previous grazing incidence X-ray scattering studies.[7] Finally, the chain orientation is shown to depend strongly on the load applied during buffing and upon the distance over which the films are buffed.

Experimental Section and Definition of Geometries

Films of poly(biphenyltetracarboxylic dianhydride-*p*-phenylenediamine) polyimide (BPDA−PDA) were prepared by spin coating solutions of the corresponding amic acid ester in *N*-methylpyrrolidinone onto 1 in. diameter Si (100) wafers. The amic acid ester films were then heated to 80 °C to remove most of the solvent. The samples were transferred to a hot plate and gradually heated to 300 °C under flowing nitrogen to cycloimidize the polymer. After cooling to room temperature, the films were buffed by passing a velour cloth under the film using a constant load that ranged from 1 to 12.5 g/cm^2 over distances ranging from 2.5 to 300 cm. A schematic diagram of the buffing geometry is shown in Figure 1a.

A schematic picture of a polyimide chain is given in Figure 1b. If we define a monomer unit as the BPDA−PDA squence in the dashed box in Figure 1c, then a chain consists of rigid monomer segments with a flexible coupling between these segments. The chain orientation is then reflected by the average segment orientation, and in the following we shall use the terms "segment orientation" and "chain orientation" synonymously. For a fully stretched chain, all monomer axes are parallel to the chain axis, as shown in the figure.[17] Within a monomer unit, or for a fully stretched chain, all atoms in the BPDA units lie in a plane (BPDA plane). The π systems of the phenyl ring and the C═O bonds are perpendicular to the BPDA plane, and they are perpendicular to the monomer axis. As shown in Figure 1d, the PDA plane is rotated about the chain axis by an angle $\delta \simeq 60°$ relative to the BPDA plane.[17] The BPDA and PDA π systems are therefore also rotated ≃60° relative to each other, and the plane spanned by the two π vectors is perpendicular to the monomer axis.

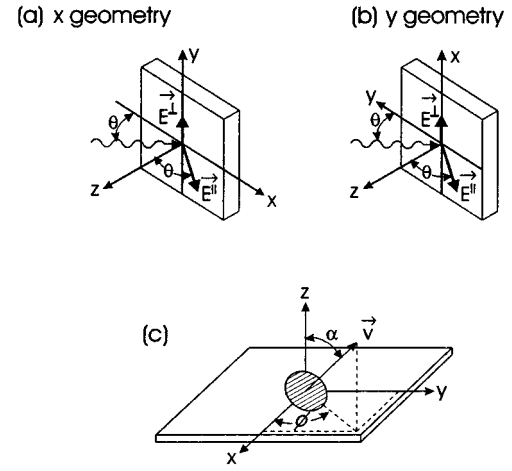

Figure 2. Coordinate system describing the experimental geometries used to record the NEXAFS spectra. The sample coordinate system is chosen with the buff direction along the *x* axis and the sample normal along the *z* axis. The X-rays are incident in the *x*−*z* plane in the "*x* geometry" (depicted in (a)) and in the *y*−*z* plane in the "*y* geometry" (depicted in (b)). The X-ray incidence angle, θ, is measured from the sample surface. The electric field vector of the circularly polarized X-rays has two components, $\vec{E}^{\parallel}$ (major) and $\vec{E}^{\perp}$. The polar angle θ of the dominant component $\vec{E}^{\parallel}$ from the surface normal is the same as the X-ray incidence angle. At non-normal X-ray incidence, the component $\vec{E}^{\parallel}$ in the *x* and *y* geometries lies parallel and perpendicular to the buff direction, respectively. (c) Specification of bond directions or axes in the polyimide chain, characterized by a vector $\vec{v}$, in terms of a polar angle α and azimuthal angle ϕ relative to the sample coordinate system.

The NEXAFS measurements were performed at the Stanford Synchrotron Radiation Laboratory (SSRL) on beam line 10-1, which delivers soft X-ray radiation from a 15 period wiggler. This beam line is equipped with a spherical grating monochromator. The entrance and exit slits were set at 20 μm to achieve an energy resolution of ≃60 meV at 300 eV. The NEXAFS data were collected simultaneously by TEY and AEY detection. The TEY was obtained by measuring the sample current with a Keithley 427 current amplifier. The AEY was measured with a cylindrical mirror analyzer (CMA). For the C and O K-edge spectra, the kinetic energy windows were positioned on the respective Auger peaks at 254 eV (width 4 eV) and 507 eV (width 8 eV), respectively. The data were normalized by the signal from a reference monitor consisting of the photocurrent from a high-transmission (85%) grid which was freshly coated with gold. The data analysis involved subtraction of a linear pre-edge background function followed by renormalization of the spectra to a constant edge jump, arbitrarily set to 1, far above the edge. The latter procedure ensured that all spectra are normalized to the same number of atoms. Prior to the measurements described here, the polyimide films were tested for radiation damage by comparing successive NEXAFS scans of short duration. The tests gave no indication of any degradation of polyimide films caused by exposure to X-rays under the conditions used in this work.

Schematics a and b of Figure 2 show the experimental geometry. The sample coordinate system is defined with the buff direction along the *x* axis and the sample normal along the *z* axis. NEXAFS spectra were recorded in two geometries, shown in Figure 2a,b, by cutting each sample wafer into two pieces, and these halves were mounted onto a sample holder with their buff directions orthogonal to each other. In the "*x* geometry" and "*y* geometry", respectively, the X-rays were incident in the *x*−*z* and *y*−*z* planes, at an incidence angle θ measured from the surface of the sample. In our case, the synchrotron radiation was elliptically polarized with a degree of linear polarization $P = 0.87$.[13,16] The dominant component $\vec{E}^{\parallel}$ of the electric field vector $\vec{E}$ was in the plane of incidence,

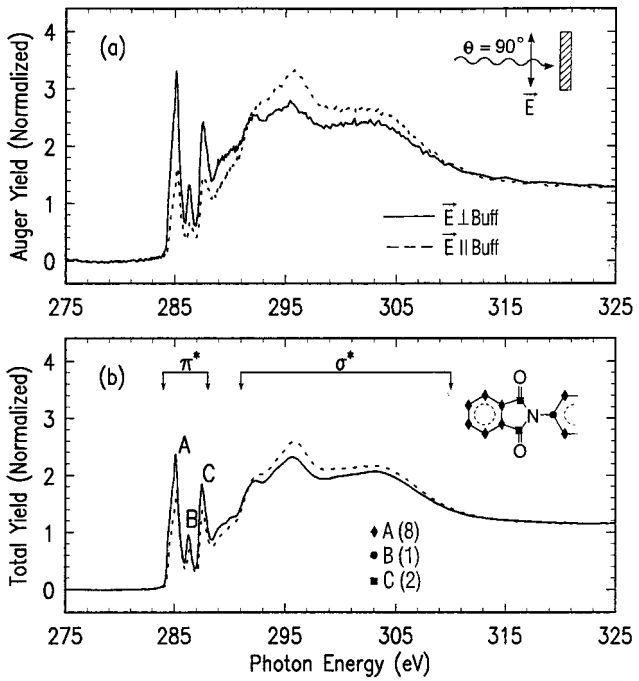

Figure 3. Carbon K-edge Auger (a) and total electron (b) yield spectra from a 1000 Å polyimide film buffed under 2 g/cm^2 for 300 cm. The X-ray incidence angle was 90°. The dashed and solid curves are spectra recorded in *x* and *y* geometries, respectively. The inset represents half of the repeat unit in the polyimide chain.

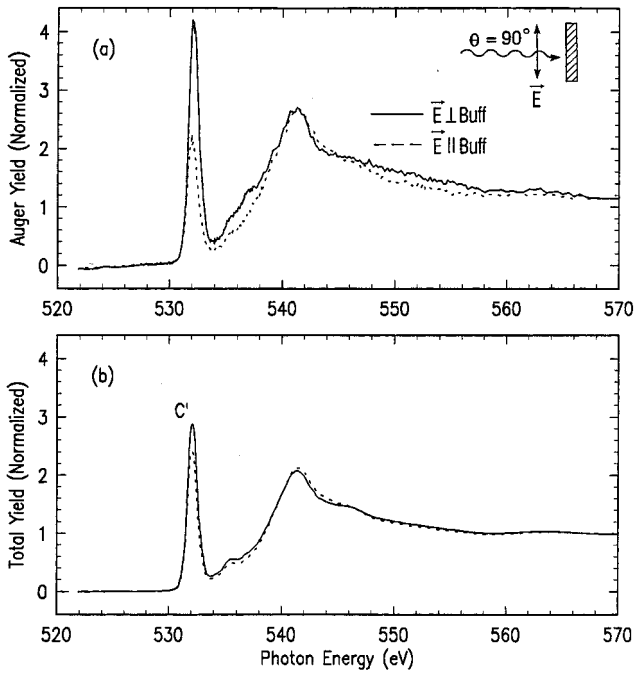

Figure 4. Oxygen K-edge Auger (a) and total electron (b) yield spectra from 1000 Å polyimide film buffed under 2 g/cm^2 for 300 cm. The X-ray incidence angle was 90°. The dashed and solid curves are spectra recorded in *x* and *y* geometries, respectively.

and the minor component $\vec{E}^{\perp}$ was perpendicular to the plane of incidence. In the *x* and *y* geometries the dominant $\vec{E}$ component $\vec{E}^{\parallel}$ was therefore parallel and perpendicular to the buff direction, respectively. NEXAFS spectra were obtained as a function of X-ray incidence angle θ, and the corresponding NEXAFS intensities will be denoted as $I_x(\theta)$ and $I_y(\theta)$, respectively.

NEXAFS spectroscopy can determine the orientation of various bond orbitals[13,16] within the polyimide chain relative to the sample coordinate system. For example, it can determine the orientation of the π orbital in the C=O group relative to the buff direction. From the orientation of the orbitals the chain orientation may then be determined. Below we shall use the polar and azimuthal angles α and ϕ defined in Figure 2c to describe the orientation of the bond orbitals in the coordinate system of the sample.

Experimental Results

Figure 3 shows carbon K-edge NEXAFS spectra at an incidence angle of 90° for a 1000 Å thick polyimide film buffed under a load of 2 g/cm^2 and 300 cm buffing distance at 1 cm/s. The intensities of various resonances in both AEY and TEY spectra are strongly influenced by the orientation of $\vec{E}$ relative to the buff direction. The first three sharp peaks, labeled A, B, and C at approximately 285.3, 286.5, and 287.7 eV, respectively, are π^* resonances corresponding to bonds associated with specific C atoms[13] as indicated in Figure 3. The peak assignments are linked to the chemical structure (corresponding to one-half of the repeat unit) in the inset. Peak A is associated with 12 C atoms/monomer in the two benzene rings within the BPDA group and the central 4 C atoms/monomer in the PDA group, peak B arises from the 2 C atoms (bonded to N) in the PDA group, and peak C is due to the 4 carbonyl C atoms/monomer. Close inspection of peak A shows that it is composed of at least three peaks arising from the chemical inequivalence of the 16 C atoms contributing to the peak. The other broad features at higher energies are transitions to the σ^* orbitals.[13] Similar spectral features are observed in both AEY and TEY, demonstrating consistency between both these detection methods. The better statistics in the TEY spectra is due to a higher signal. The spectral differences between the *x* and *y* geometries clearly demonstrate a preferred orientation of the polyimide chains within the sample. In particular, the π^* and σ^* structures have opposite polarization dependence, as expected.

Figure 4 shows spectra obtained at the oxygen K-edge recorded on the same sample as for Figure 3, at an incidence angle of 90°. The AEY and TEY data show similar features and trends. The sharp resonance peak C′ at ≃532.0 eV originates from a transition to the π^* orbital of the carbonyl group, and therefore corresponds to peak C in the carbon K-edge spectra. The features at higher energies correspond to the carbonyl group σ^* resonances. The π^* intensities of the carbonyl resonances are higher in the *y* than the *x* geometry at both carbon and oxygen edges, indicating consistency between these measurements.

A comparison of carbon K-edge spectra obtained in the *x* and *y* geometries at incidence angles of 20° is shown in Figure 5. The shape and position of various resonances in these spectra are consistent with those in Figure 3. Within the accuracy of the measurements, the intensities recorded for the two geometries in Figure 5 are identical. The same observation holds for the oxygen K-edge spectrum recorded at 20° incidence angle, shown in Figure 6. In general, the π^* (σ^*) resonances recorded at 20° X-ray incidence are larger (smaller) than those recorded at 90°.

The π^* resonances are sharp and lie at energies below the 1s ionization potential of carbon (≃290 eV). Thus their intensities can be determined quite accurately. The multiple π^* resonances not only allow precise determination of the π orbital orientations within the various groups but also provide an internal consistency check. Since the intensity analysis of peak A is most reliable,

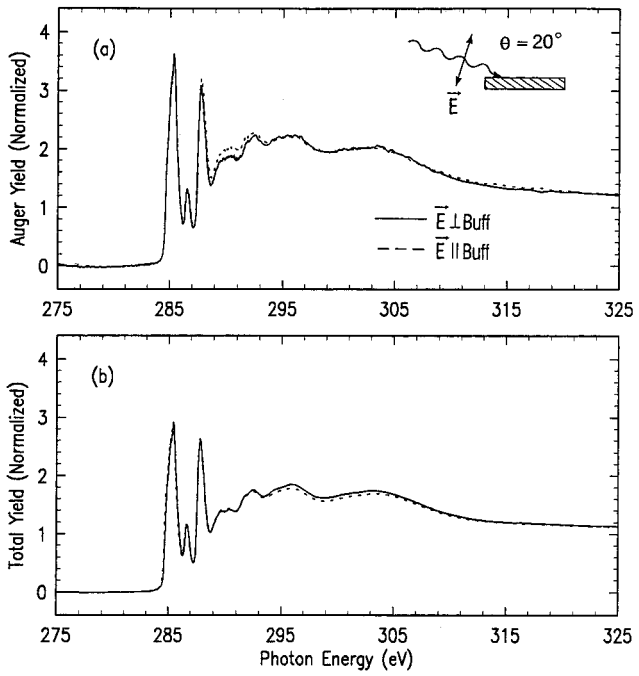

Figure 5. Carbon K-edge Auger (a) and total electron (b) yield spectra from 1000 Å polyimide film buffed under 2 g/cm^2 for 300 cm. The X-ray incidence angle was 20°. The dashed and solid curves are spectra recorded in *x* and *y* geometries, respectively.

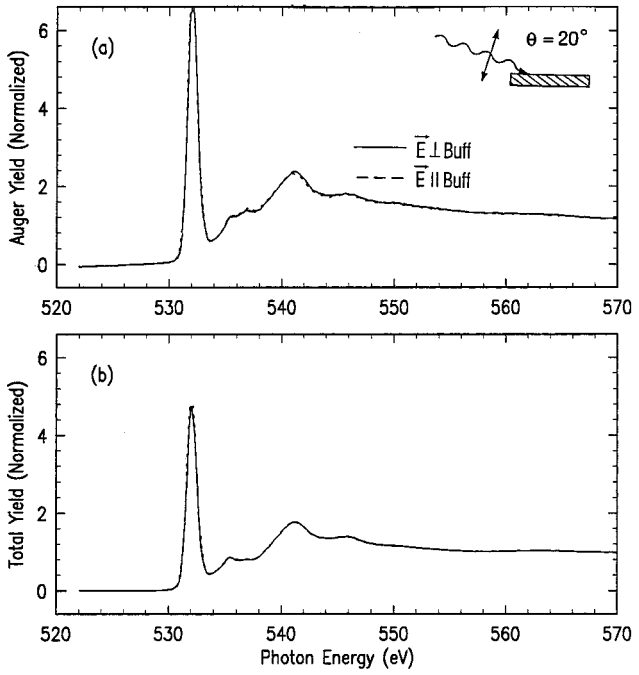

Figure 6. Oxygen K-edge Auger (a) and total electron (b) yield spectra from 1000 Å polyimide film buffed under 2 g/cm^2 for 300 cm. The X-ray incidence angle was 20°. The dashed and solid curves are spectra recorded in *x* and *y* geometries, respectively.

it has been used preferentially for the determination of the chain orientation. While σ^* resonances can also be used to measure the chain orientation, their analysis is complicated by the fact that they are broad and superimposed on a background which limits the determination of peak intensities.

A plot of the intensity of peak A as a function of X-ray incidence angle θ for AEY and TEY detection in the *x* and *y* geometries is shown in Figure 7. Since the peak shape of each resonance is independent of incidence

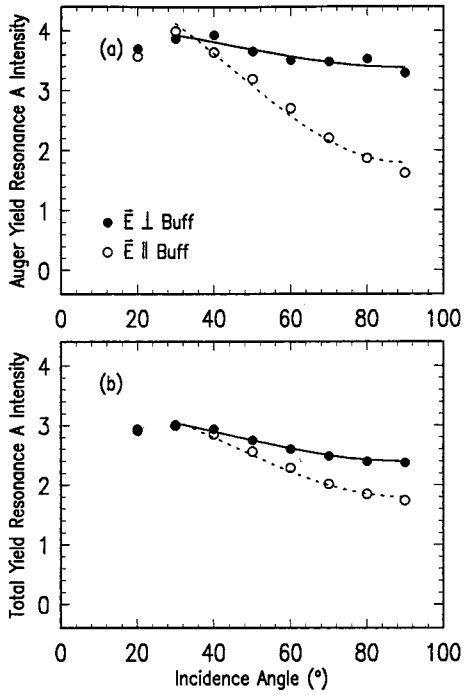

Figure 7. Comparison of π^* resonance intensities for peak A at 285.3 eV in *x* and *y* geometries as a function of X-ray incidence angle θ. The sample was a 1000 Å polyimide film buffed under a load of 2 g/cm^2 for 300 cm. Both AEY (a) and TEY (b) results are shown. Dashed and solid curves are fits to eq 1 for the two indicated geometries.

angle, the peak intensities can be accurately represented by peak heights. For peaks A and C′ the peak heights were directly taken from the spectra without background correction. For peaks B and C the peak heights were corrected for a background which was assumed to be linear in the regions 284.3−287.2 and 287.2−288.5 eV, respectively. The intensities plotted in Figure 7 were obtained for the polyimide sample buffed under a load of 2 g/cm^2 to a distance of 300 cm. For the sake of clarity, only the intensity for peak A is plotted. The other π^* resonances B, C, and C′ at 286.5, 287.65, and 532 eV showed similar trends. The solid and dashed lines are fits to these data, using angle-dependent functions discussed below.

Angular Dependence of NEXAFS Intensities

In the following, we shall discuss how the measured angular dependence of the intensities of peaks A−C′ can be used to determine the preferred orientation of the polyimide chains. It is important to realize that, in contrast to X-ray diffraction, NEXAFS does not require order, that is a correlation of chains relative to each other. Because the X-ray absorption process occurs on a single atom, NEXAFS measures the orientation of bonds associated with that atom. For polyimide the average orientation of the π orbitals of the C atoms in the various phenyl rings and in the C=O unit is determined. In particular, we determine the average orientation of the BPDA and PDA π systems. Refering to Figure 1c, we see that for each monomer unit the π orbitals are oriented perpendicular to the monomer axis. The problem of determining the chain orientation therefore reduces to determining the orientation of the monomer axis from the orientation of the π systems. In the following, we shall therefore discuss how the orientation of the π systems can be used to determine the orientation of the monomer axis.

If the phenyl rings within a monomer unit were free to spin (assume all orientations) about the monomer axis, then the π orbitals define a plane perpendicular to the monomer axis. The monomer axis is then uniquely defined as the normal to the π orbital plane, and the monomer axis and the chain axis, i.e. the average of all monomer axes, can be determined from the measured angular dependence of the π^* NEXAFS intensities, using the equations for the "plane" case given in refs 13 and 16 (see below). Similarly, in this case, the chain axis can also be determined from the angular dependence of the σ resonances associated with the phenyl rings since a spinning phenyl ring has the largest σ orbital projection along the rotation axis. This situation corresponds to the "vector" case described in refs 13 and 16 (see below).

On the other hand, if the phenyl rings and the C═O bonds, and therefore their π systems, on average, have a preferred orientation in a plane perpendicular to the chain axis (e.g. parallel to the surface), the direction of the chain axis is not uniquely defined relative to a given π system but can lie anywhere in the plane perpendicular to the π bond direction. In this case, the chain axis cannot be determined from the angular dependence of a single π^* resonance intensity alone. However, Figure 1d shows that within each monomer unit the ring planes and π systems of the BPDA and PDA units are not collinear, e.g. include an angle of 60° for a fully stretched chain. The π systems of the two structural units therefore span a plane perpendicular to the chain axis. Thus, if one could spectroscopically separate the π^* intensities of the BPDA or C═O groups (which have parallel π systems) from those of the PDA groups, one could combine the results to determine the average segment orientation. As shown in the previous section, resonances A, B, and C in Figure 3 are indeed associated with different π systems in the phenyl and C═O groups and, as shown below, can be combined to derive the direction of the chain axis relative to the buff direction.

The angular dependence of the measured NEXAFS intensities is governed by the following general equation:[13]

$$I_i = PI_i^{\parallel} + (1 - P)I_i^{\perp} \quad (1)$$

where $i = x$ or y and P is a polarization factor which in our case has the value $P = 0.87$. $I^{\parallel}$ and $I^{\perp}$ are intensities corresponding to the parallel and perpendicular components of the E vector, as illustrated in Figure 2a,b. Since it is not *a priori* clear whether the BPDA and PDA planes are azimuthally oriented in a plane perpendicular to the chain axis, we have analyzed the angular dependence of the resonance intensities A−C′ in two ways. First, we assumed uniaxial symmetry, i.e., on average, cylindrical symmetry, about the chain axis. As mentioned above, in this case the π system defines a plane perpendicular to the chain axis, and the angular dependence of the π^* intensities can be described by the equations for an orbital "plane"[13,16]

$$I_x^{\parallel} = B[1 - \cos^2\theta\cos^2\alpha - \sin^2\theta\sin^2\alpha\cos^2\phi] \quad (2a)$$

$$I_y^{\parallel} = B[1 - \cos^2\theta\cos^2\alpha - \sin^2\theta\sin^2\alpha\sin^2\phi] \quad (2b)$$

$$I_x^{\perp} = B[1 - \sin^2\alpha\sin^2\phi] \quad (3a)$$

$$I_y^{\perp} = B[1 - \sin^2\alpha\cos^2\phi] \quad (3b)$$

Table 1

resonance (energy)	detection method	I_x/I_y ($\theta = 90°$)	ϕ, deg	α, deg	R_{xy}
A (285.3 eV)	AEY	0.526	57.4	41	−0.42
B (286.5 eV)	AEY	0.478	59.3	49	−0.48
C (287.7 eV)	AEY	0.549	56.6	34	−0.39
C′ (532 eV)	AEY	0.541	56.7	37	−0.40
A (285.3 eV)	TEY	0.758	50.4	51	−0.19
B (286.5 eV)	TEY	0.719	51.4	66	−0.22
C (287.7 eV)	TEY	0.752	50.5	46	−0.19
C′ (532 eV)	TEY	0.870	47.7	30	−0.09

where B is a constant, θ is the X-ray incidence angle, and ϕ and α specify the azimuthal and polar angles of the normal to the π orbital plane, i.e. the chain direction, in the coordinate system of the sample, as shown in Figure 2c. We were unsuccessful in fitting the data shown in Figure 7 with the above angular dependence, indicating that the phenyl rings in the polyimide chains do not possess a uniaxial distribution about the chain axis. This result may be expected near the surface of a film where the symmetry is broken by the surface.

In our second analysis we assumed that the π systems of the chain, on average, show a preferred orientation in the plane perpendicular to the chain axis. In this model the orientation of the different π systems is described by the vector $\vec{\nu}$ in Figure 2c, again characterized by a polar angle α and an azimuthal angle ϕ in the coordinate system of the sample. The relevant equations for the NEXAFS intensities are[13,16]

$$I_x^{\parallel} = C[\cos^2\theta\cos^2\alpha + \sin^2\theta\sin^2\alpha\cos^2\phi] \quad (4a)$$

$$I_y^{\parallel} = C[\cos^2\theta\cos^2\alpha + \sin^2\theta\sin^2\alpha\sin^2\phi] \quad (4b)$$

$$I_x^{\perp} = C\sin^2\alpha\sin^2\phi \quad (5a)$$

$$I_y^{\perp} = C\sin^2\alpha\cos^2\phi \quad (5b)$$

where C is a constant.

The corresponding fit is shown in Figure 7 and the resonance intensities at $\theta = 90$ and 60° were used to determine the angles ϕ and α for each π^* orbital. The results are listed in Table 1.

As mentioned above, the orientation of a single π system does not uniquely define the orientation of the chain axis. However, inspection of Table 1 shows that, within experimental error, the resonance intensities associated with peaks A−C yield the same angles $\phi = 58 \pm 1.5°$ for the AEY data and $\phi = 51 \pm 1°$ for the TEY data. Here ϕ describes the in-surface-plane orientation of the corresponding π orbitals relative to the buff direction. The π systems associated with peaks A−C therefore all lie in the plane defined by the z axis and the line $\phi = 58°$ (51° for TEY) in the $x-y$ plane. In the following, we shall refer to this plane as the π plane. Since the chain axis is perpendicular to the π plane, it lies in the $x-y$ surface plane at an angle $90° - \phi$ or 32° (39° for TEY) from the buffing direction. According to Table 1, the π systems associated with peaks A−C are oriented at different polar angles α within the π plane. This may be understood from Figure 1d, which shows that for a fully stretched chain the different π systems are tilted by $\delta = 60°$ relative to each other. The observed angles for α vary by less than 20°, indicating that there is substantial disorder in the orientation of the BPDA and PDA π systems relative to each other.

Without discussing details, we would like to mention that the angular dependence of the σ^* resonances confirms the results obtained from the analysis of the π^* intensities. The angular dependence of the σ^* intensities, however, is described by eqs 2 and 3, since the C−C bonds in the phenyl rings span a plane. The orientation of the normal of that plane is then described by the same angles α and ϕ as the π orbitals of the rings.

Distribution Function, Orientation Function, and Dichroic Ratio

In the previous section we have related the angle-dependent intensities of NEXAFS resonances to the orientation angles ϕ and α of the π systems of the BPDA and PDA groups in the coordinate system of the sample. The question arises as to what these angles really mean for a partially disordered system like a polymer film. In general, one would like to determine the actual angular distribution function $D(\gamma,\psi)$ of the polymer units in the coordinate system of the sample, where the spherical angles γ and ψ are taken relative to the z axis and x axis, respectively. Unfortunately, $D(\gamma,\psi)$ cannot be uniquely determined from the NEXAFS data. Instead, the NEXAFS intensities $I_i(\alpha,\phi,\theta)$, measured for $\vec{E}^{\parallel}$ along the $i = x$ and y axes, respectively, are determined by the convolution of $D(\gamma,\psi)$ and the intensity distribution function $I_i(\gamma,\psi,\theta)$ (i.e. eqs 4 and 5 with $\phi = \psi$ and $\alpha = \gamma$) according to

$$I_i(\alpha,\phi,\theta) = \frac{\int_0^{2\pi}\int_0^{\pi} I_i(\gamma,\psi,\theta)\, D(\gamma,\psi) \sin\gamma \, d\gamma \, d\psi}{\int_0^{2\pi}\int_0^{\pi} D(\gamma,\psi) \sin\gamma \, d\gamma \, d\psi} \quad (6)$$

The easiest way to visualize the information contained in the measured NEXAFS intensity distribution function $I(\alpha,\phi,\theta)$ is to assume that all polymer chains are fully stretched and aligned along the direction specified by α and ϕ. In this case $D(\gamma,\psi)$ is expressed by a δ distribution function,

$$D(\gamma,\psi) = \delta(\phi-\psi,\alpha-\gamma) \quad (7)$$

Instead of assuming the same alignment of all N_{tot} chains, specified by angles α and ϕ, one would obtain the same result if one assumed that fractions $N_x/N_{tot} = \cos^2\phi \sin^2\alpha$, $N_y/N_{tot} = \sin^2\phi \sin^2\alpha$, and $N_z/N_{tot} = \cos^2\alpha$ of chains were aligned along the x, y, and z axes, respectively, a case expressed by the orientation function,

$$D(\gamma,\psi) = \frac{N_x}{N_{tot}}\delta(0°-\psi,90°-\gamma) + \frac{N_y}{N_{tot}}\delta(90°-\psi,90°-\gamma) + \frac{N_z}{N_{tot}}\delta(0°-\gamma) \quad (8)$$

The fact that the orientation functions given by eqs 7 and 8 lead to the same measured intensity distribution $I(\alpha,\phi,\theta)$, i.e. to the same orientation angles α and ϕ, demonstrates that $D(\gamma,\psi)$ cannot be uniquely determined by NEXAFS.

For buffed polymer surfaces, the in-plane alignment relative to the buffing direction is of particular interest and one would like to obtain the two-dimensional distribution function $f(\psi)$ in the $x-y$ plane. In the following, we shall assume that the three-dimensional distribution function is separable, according to $D(\gamma,\psi) = f(\psi)\, h(\gamma)$ so that we can consider the in-plane distribution separate from the out-of-plane distribution. It is clear that for a polymer film $f(\psi)$ will be far from the δ-like distribution function, and it is reasonable to assume that, to lowest order, it has the form

$$f(\psi) = A\cos^2\psi + B\sin^2\psi \quad (9)$$

$f(\psi)$ gives the number of bonds or chain segments aligned in the direction ψ measured from the buffing direction (x axis). According to eqs 4−6, the NEXAFS intensities corresponding to $\vec{E}^{\parallel}$ along the x and y axes ($\theta = 90°$) are then given by

$$I_x^{\parallel}(\phi) = I_y^{\perp}(\phi) = C'\cos^2\phi = \frac{C'\int_0^{2\pi}\cos^2(\psi)\, f(\psi)\, d\psi}{\int_0^{2\pi} f(\psi)\, d\psi} = C'\frac{3A+B}{4(A+B)} \quad (10)$$

and

$$I_y^{\parallel}(\phi) = I_x^{\perp}(\phi) = C'\sin^2\phi = \frac{C'\int_0^{2\pi}\sin^2(\psi)\, f(\psi)\, d\psi}{\int_0^{2\pi} f(\psi)\, d\psi} = C'\frac{A+3B}{4(A+B)} \quad (11)$$

where $C' = C\sin^2\alpha$. With the normalization $\int_0^{2\pi} f(\psi)\, d\psi = \pi(A+B) = 1$, we can determine values for A and B from the measured NEXAFS intensities $I_x(\phi)$ and $I_y(\phi)$ (see below).

One may also use the measured NEXAFS intensities to define an orientation function as is commonly done.[18] The use of an orientation function has the advantage that it is simply defined by the measured intensities without knowledge of the actual distribution function. In practice, however, only uniaxial orientation functions have been determined as discussed in ref 18. Since it is clear from the above discussion that a rubbed polyimide surface is not a uniaxial system, it is more appropriate to use a dichroic ratio to describe the preferential alignment. The alignment in the $x-y$ surface plane is then described by the dichroic ratio[12]

$$R_{xy} = \frac{I_x^{\parallel} - I_y^{\parallel}}{I_x^{\parallel} + I_y^{\parallel}} = \frac{I_x - I_y}{(I_x + I_y)(2P-1)} = \cos^2\phi - \sin^2\phi \quad (12)$$

where I_y and I_x are the measured intensities in the x and y geometries at an incidence angle of 90°, using X-rays with a degree P of linear polarization. It is seen that R_{xy} is sensitive only to the in-plane orientation of the polyimide chains, and thus it provides a useful criterion for the degree of alignment relative to the buffing direction. Since we use the intensities of the π^* resonances which are oriented normal to the chain axis in determining R, a preferred chain orientation along the buffing direction will be manifested by negative values of R. R varies from −1, for perfect alignment along the buffing direction, to 1, for perfect alignment perpendicular to the buffing direction. For completely random orientation $R = 0$. In analogy to eq 8, one may visualize the preferred chain orientation as a larger fraction $N_x/N_{tot} = (1 - R_{xy})/2$ of perfectly aligned chains parallel to the buff direction than the fraction $N_y/N_{tot} = (1 + R_{xy})/2$ of chains that are perfectly aligned perpendicular to the buffing direction. By assuming a

more realistic distribution function of the form given by eq 9, one can relate R_{xy} to the parameters A and B according to

$$R_{xy} = \frac{A - B}{2(A + B)} \tag{13}$$

The results of the dichroic ratio analysis for the various π^* resonances are given in Table 1. The values for the weak resonance B should have the largest error bars, and if we exclude this, we obtain averaged values $\phi = 57°$ for AEY and 50.5° for TEY detection for resonances A, C, and C′. These values yield $R_{xy} = -0.41$ for AEY and -0.19 and TEY, respectively. When converted into a distribution function according to eq 9, one obtains $A = 0.09$ and $B = 0.91$ (AEY) and $A = 0.31$ and $B = 0.69$ (TEY), reflecting a pronounced angular distribution pattern with preference of the π system to align along the y axis, i.e. the chain axis to align along the buffing direction x.

Similarly, we can describe the alignment of the π system in the plane perpendicular to the chain axis, defined by the z axis and an in-plane axis y' (intercept of the π plane with the $x-y$ plane) by the dichroic function

$$R_{zy'} = \frac{I_z^{\parallel} - I_{y'}^{\parallel}}{I_z^{\parallel} + I_{y'}^{\parallel}} = \cos^2 \alpha - \sin^2 \alpha \tag{14}$$

where $I_z^{\parallel}$ and $I_{y'}^{\parallel}$ are the intensities for X-rays incident along the chain axis with $\vec{E}^{\parallel}$ along the z and y' axes, respectively. The best measure of $R_{zy'}$ is obtained from the intensities of resonances C and C′, corresponding to the C=O π bonds. Resonance A has contributions from atoms in both the BPDA and PDA units, and its interpretation is therefore more complicated. Resonance B originates only from atoms in the PDA group but its intensity is small, resulting in larger error bars. Using the averaged α value for peaks C and C′, we obtain $\alpha = 35.5°$ for AEY and 43° for TEY and the corresponding values $R_{zy'} = 0.33$ (AEY) and 0.07 (TEY).

Discussion

Chain Axis Orientation. From the above discussion it is clear that after buffing, the polyimide chains are preferentially aligned along the buffing direction. This result may be visualized in three different ways as illustrated in Figure 8. Here we show three different distribution functions which specify the alignment in the $x-y$ plane. The functions are those corresponding to eqs 7−9 and, as discussed earlier, are all consistent with our experimental NEXAFS results. They therefore represent different ways to picture our results. The first distribution function, shown in Figure 8a,b for the AEY and TEY results, respectively, is based on a model where all chains are aligned in the surface plane at an angle $90 - \phi = 33°$ (AEY) and 39.5° (TEY) from the buffing direction. The second distribution function shown in Figure 8c,d is closely related to the dichroic ratio R_{xy}. In this model, a fraction $(1 - R_{xy})/2 = 0.7$ (AEY) and 0.6 (TEY) of the chains is parallel to the buff direction and a fraction $(1 + R_{xy})/2 = 0.3$ (AEY) and 0.4 (TEY) is aligned perpendicular to the buff direction. Finally, we show in Figure 8e,f a continuous distribution given by eq 9, where fractions $A = 0.09/\pi$ and $B = 0.91/\pi$ (AEY) and $A = 0.31/\pi$ and $B = 0.69/\pi$ (TEY) of the chains are aligned perpendicular and parallel to the buffing direction. The larger alignment observed by means of AEY detection is a consequence of the smaller probing depth, and it signifies that the alignment is highest at the surface and decays into the bulk, as discussed in more detail below.

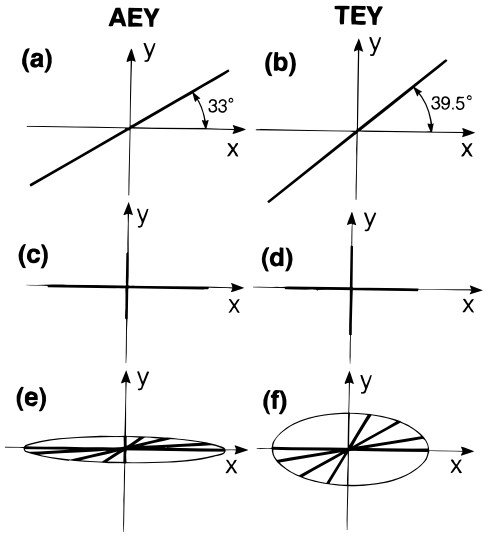

Figure 8. Plot of three simple in-plane distribution functions describing the chain orientation relative to the buffing direction x. All three distributions are consistent with the NEXAFS data recorded with Auger electron yield (AEY) and total electron yield (TEY) detection, respectively, and serve to visualize the results. Plots a and b show a δ-like distribution (eq 7) assuming that all chain segments and therefore chains are aligned along a specific azimuthal angle ϕ from the buffing direction. Plots c and d assume a model with two discrete orthogonal chain orientations (eq 8) along the x and y axes, respectively. Plots e and f assume a continuous distribution of chain segments according to eq 9, which has a maximum along the buffing direction x and a minimum along y. The total number of chains in (e) and (f) corresponds to the area inside the ellipse-like curve and is therefore a factor of π larger than that in (a)−(d).

Orientation of π Systems about the Chain Axis. Besides determining the orientation of the chain axis in the surface plane, it is of considerable interest to learn about the orientation of the phenyl and C=O π systems relative to the surface normal, which always constitutes a unique axis in a thin film. This problem is addressed by eq 14, which defines a dichroic ratio in the plane perpendicular to the chain axis. From Table 1 it is evident that resonances A−C′ lead to different values for the alignment angle α of the π systems with the surface normal. This is to be expected since the resonances correspond to different π systems. As stated earlier, the resonance at 285.3 eV includes contributions from 16 C atoms (12 from the BPDA unit and 4 from the PDA unit). Since the total intensity of resonance A is the sum of the intensity contributions from each C atom, the polar angle α_A should be related to the polar angles α_{BPDA} and α_{PDA} of the corresponding phenyl groups according to

$$16 \cos^2 \alpha_A = 12 \cos^2 \alpha_{BPDA} + 4 \cos^2 \alpha_{PDA} \tag{15}$$

Here $\alpha_{BPDA} = \alpha_{C=O} = 35.5°$ is determined from peak C and $\alpha_{PDA} = 49°$ from peak B. We obtain $\alpha_A = 39°$, which is in agreement with the measured value of $41 \pm 2°$. From the TEY results a higher polar angle $\alpha_{BPDA} = \alpha_{C=O} = 46 \pm 2°$ is obtained, which reflects the loss of orientation with increasing distance from the surface. Using $\alpha_{PDA} = 66°$, eq 15 predicts $\alpha_A = 51°$, in good agreement with the measured value of $49 \pm 2°$ (Table 1).

As discussed earlier, the value $\alpha_{C=O}$ is best suited to obtain a measure of the alignment in the π plane. The values $\alpha_{C=O} = 35.5°$ obtained from peaks C and C′ for AEY and 43° for TEY yield $R_{zy'} = 0.33$ (AEY) and 0.07 (TEY), respectively. These dichroic ratios are of similar magnitude as those for the in-plane chain alignment relative to the buffing direction. Our AEY results indicate a substantial alignment of the BPDA and C=O π systems along the surface normal, leading to a strong deviation from uniaxial symmetry near the surface. This alignment decreases away from the surface as indicated by the TEY results.

We note that the value $\alpha_{BPDA} = 35.5°$ is close to the setting angle of 30° in crystalline polyimide,[17] defined as the angle between the BPDA plane and the (100) planes of the crystal. In the polyimide crystal the chains are close packed in the (100) plane with the chain axis along [001]. Thus, one might correlate the surface plane of a buffed polyimide film with the (100) plane in crystalline polyimide and the buffing direction with the [001] crystalline direction.

Depth Dependence. The difference in orientation implied by the AEY and TEY results is due to the different sampling depths of these detection schemes. In our AEY measurements the escaping KVV Auger electrons have energies of 254 eV (C K-edge) and 507 eV (O K-edge) with mean free paths of 10.5 Å (254 eV) and 17 Å (511 eV) in polyimide,[15] comparable to 2−3 segment diameters. In TEY measurements the signal predominantly arises from low-energy scattered electrons, and the resulting sampling depth is considerably larger, about 100 Å for photon energies around the C K-edge.[15] Thus, using AEY detection and the C K-edge spectra, we can obtain the segment orientation at the surface. The average dichroic ratios for the C K-edge (peaks A and C in Table 1) are $R_{xy} = -0.41$ in AEY and −0.19 in TEY. From the O K-edge data (peak C′) we obtain values $R_{xy} = -0.40$ in AEY and −0.09 in TEY. This supports the argument that the degree of chain axis alignment along the buffing direction is higher at the sample surface. This is reasonable as the aligning effect of buffing should be maximum at the surface of the polymer film.

The dichroic ratio can be used to estimate the 1/e alignment depth. The above results suggest that R_{xy} varies from −0.41 at the polymer film surface to 0 deep inside the sample. If R_{xy} is assumed to vary exponentially as a function of depth, z, with D as the (1/e) orientation depth, we obtain

$$R_{xy}(z) = -0.41e^{-z/D} \tag{16}$$

With AEY detection the surface orientation is measured. Let us denote the 1/e sampling depth for TEY detection as d_{TEY}. Typically, d_{TEY} is significantly smaller than the penetration depth of X-rays and, hence, attenuation of X-rays can be ignored in the analysis. For example, at an X-ray incidence angle of 90° the (1/e) penetration depth of 310 eV X-rays (this energy corresponds to excitation into the structureless continuum above the edge) is about 2300 Å. The fraction of electrons created at depth z escaping the sample is then $e^{-z/d_{TEY}}$ and the average dichroic function R_{xy}^{TEY} corresponding to the TEY sampling depth is given as follows:

$$R_{xy}^{TEY} = \frac{\int_0^\infty e^{-z/d_{TEY}}(-0.41e^{-z/D})\,dz}{\int_0^\infty e^{-z/d_{TEY}}\,dz} \tag{17}$$

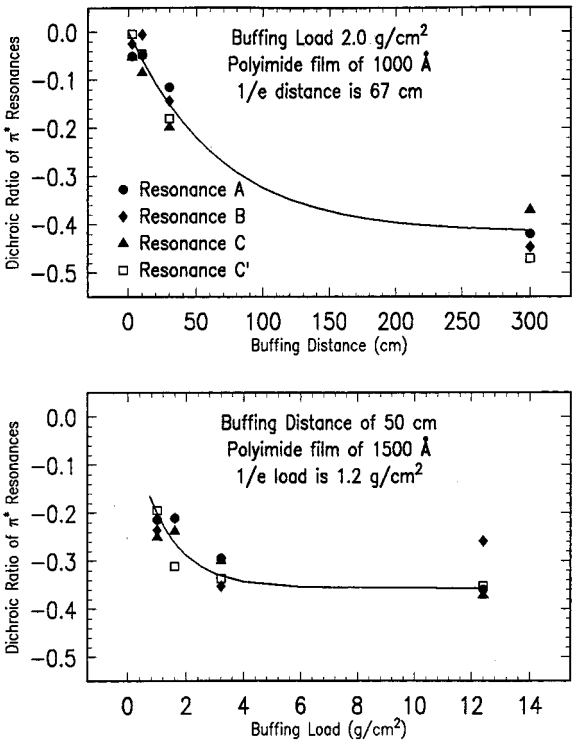

Figure 9. Plot of the dichroic ratio obtained from AEY results as a function of buffing distance and buffing load. The data points include results for all the π^* resonances. The solid curve is a fit to the data using an exponential curve.

which, after integration, yields

$$R_{xy}^{TEY} = \frac{-0.41}{1 + d_{TEY}/D} \tag{18}$$

From the experimentally determined TEY value $R_{xy}^{TEY} = -0.19$ at the C K-edge, we can determine the value $d_{TEY}/D = 1.16$, implying that the 1/e alignment depth of the polyimide film is about the same as the depth sensitivity of the total electron yield, i.e. approximately 100 Å.

Load and Distance Dependence. AEY and TEY NEXAFS spectra were also measured for samples which were buffed under a constant load to different buffing distances. The samples in this series were 1000 Å polyimide films buffed under a load of 2 g/cm² to distances of 2.5, 10, 30, and 300 cm. Secondly, we measured AEY and TEY spectra on samples which were buffed to the same distance but with differing loads. In this case the samples were 1500 Å polyimide films buffed to a distance of 50 cm under loads of 1, 1.6, 3.2, and 12.5 g/cm². The results on these samples may be used to quantitatively determine the dependence of the chain orientation on the load and distance in the buffing process. Figure 9 shows the AEY results for all π^* resonances. The dichroic ratios show an exponential dependence, indicated as solid lines in the figures, on both buffing load and distance. R is 0 for no alignment and the maximum value measured was −0.41. The 1/e buffing distance is 67 cm and 1/e load is 1.2 g/cm². Figure 10 shows a summary of the TEY data for π^* resonances A−C. Again, the solid lines are fits to the data using an exponential function. The 1/e distance is 140 cm and 1/e load is ∼2 g/cm². The data suggest that the buffing distance is a more critical parameter to achieve orientation deep into the sample since the 1/e distance for the TEY results is more than twice that for the AEY results.

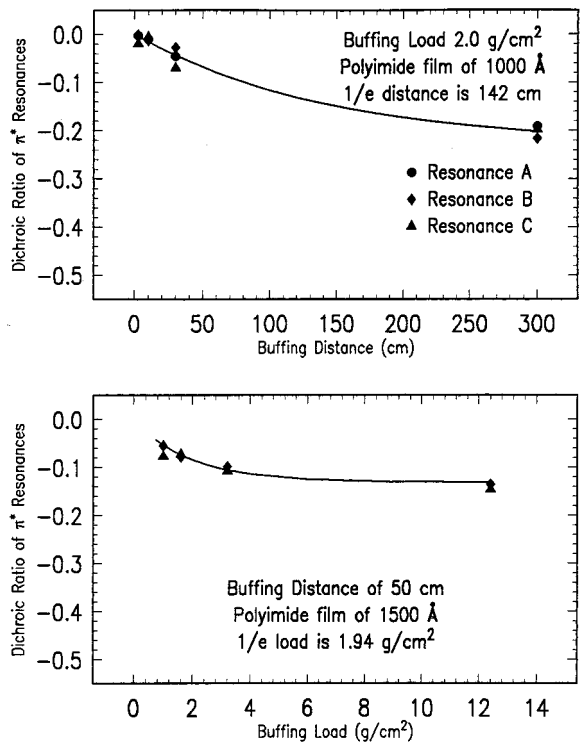

Figure 10. Same as for Figure 9 for TEY data.

Conclusions

For buffed BPDA−PDA polyimide, the NEXAFS spectra at the carbon and oxygen K-edges are strongly dependent on the relative orientation between the electric field vector of the X-rays and the buffing direction. This demonstrates a strong influence of buffing on the near-surface orientation of the polyimide chains. We find two types of orientational effects. First, the chain axis is found to lie in the surface plane with a preferential orientation along the buffing direction. The degree of orientation is quantified and pictured in three models using different angular distribution functions. We also find substantial alignment of the π systems of the BPDA, PDA, and C=O units in the plane perpendicular to the preferred chain orientation axis. At the surface the BPDA and C=O π systems, which are parallel, are preferentially aligned along the surface normal. All orientational effects are found to decrease away from the surface, decaying to zero in the bulk of the film. Based on the value of the dichroic ratio for the AEY and TEY data, the 1/e alignment depth is approximately 100 Å.

We also determined the dependence of the chain alignment on the buffing distance and the buffing load. The 1/e buffing distance estimated from the AEY data is 67 cm as compared to 142 cm determined from the TEY data. For the 1/e buffing load, we obtain 1.2 g/cm^2 from the AEY data and 2 g/cm^2 from the TEY data.

Acknowledgment. NEXAFS measurements were made at the Stanford Synchrotron Radiation Laboratory (SSRL), which is supported by the U.S. Department of Energy. This work was partially supported by the U.S. Department of Energy under Contract FG03-88ER-45375.

References and Notes

(1) Depp, S. W.; Howard, W. E. *Sci. Am.* **1993**, *268*, 90.
(2) Geary, J. M.; Goodby, J. W.; Kmetz, A. R.; Patel, J. S. *J. Appl. Phys.* **1987**, *62*, 4100.
(3) van Aerle, N. A. J. M.; Barmentlo, M.; Hollering, R. W. *J. Appl. Phys.* **1993**, *74*, 3111.
(4) van Aerle, N. A. J. M.; Tol, A. J. W. *Macromolecules* **1994**, *27*, 6520.
(5) Chen, W.; Moses, O. T.; Shen, Y. R.; Yang, K. H. *Phys. Rev. Lett.* **1992**, *68*, 1547.
(6) Zuang, X.; Marucci, L.; Shen, Y. R. *Phys. Rev. Lett.* **1994**, *73*, 1513.
(7) Toney, M. F.; Russell, T. P.; Logan, J. A.; Kikuchi, H.; Sands, J. M.; Kumar, S. K. *Nature* **1995**, *374*, 709.
(8) Kochi, M.; Horigomi, T.; Mita, I. *Recent Advances in Polyimide Science and Technology, 192*; Weber, W. D., Gupta, M. R., Eds.; Society of Plastics Engineers: New York, 1987.
(9) Brown, H. R.; Russell, T. P. *Macromolecules* **1996**, *29*, 798.
(10) Reiter, G. *Eur. Phys. Lett.* **1992**, *23*, 579.
(11) Keddie, J. L.; Jones, R. A. L.; Cory, R. A. *Europhys. Lett.* **1994**, *27*, 59.
(12) Orts, W. J.; van Zanten, J. H.; Wu, W. L.; Satija, S. K. *Phys. Rev. Lett.* **1993**, *71*, 867.
(13) Stöhr, J. *NEXAFS Spectroscopy*; Springer Series in Surface Sciences 25; Springer-Verlag: Berlin, 1992.
(14) Ade, H.; Zhang, X.; Cameron, S.; Costello, C.; Kirz, J.; Williams, S. *Science* **1992**, *258*, 972.
(15) The Auger sampling depth is simply the inelastic mean free path given for polyimide by Tanuma et al. (Tanuma, S.; Powell, C. J.; Penn, D. R. *Surf. Interface Anal.* **1993**, *21*, 165). It is 10.5 Å for 254 eV (carbon KLL) and 17 Å for 507 eV (oxygen KLL) Auger electrons. The total electron yield sampling depth L can be determined from the quantum yield Y_0 according to $L = Y_0/\mu_x(h\nu)$, where $\mu_x(h\nu)$ is the linear X-ray absorption coefficient (unit 1/length). $\mu_x(h\nu) = \mu(h\nu)\rho$, where $\mu(h\nu)$ is the mass absorption coefficient (units cm^2/g) and ρ is the mass density (units g/cm^3). Using the value $Y_0/h\nu\mu(h\nu) = 7 \times 10^{-9}$ g/cm^2 eV for vitreous carbon given in Figure 10 in Day et al. (Day, R. H.; Lee, P.; Saloman, E. B.; Nagel, D. J. *J. Appl. Phys.* **1981**, *52*, 6965) and $\rho = 2$ g/cm^3, we obtain $L \simeq 100$ Å for $h\nu = 300$ eV.
(16) Stöhr, J.; Outka, D. A. *Phys. Rev. B* **1987**, *36*, 7891.
(17) Ree, M.; Yoon, D. Y.; Depero, L. E.; Parrish, W., in preparation.
(18) *Structure and Properties of Polymers*; Ward, I. M., Ed.; J. Wiley and Sons: New York, 1975; Chapters 1, 4.

MA951820C